A Depolarizing Chipless RF Label for Dielectric Permittivity Sensing

Filippo Costa, *Member, IEEE*, Antonio Gentile, Simone Genovesi, *Member, IEEE*, Luca Buoncristiani, Antonio Lazaro, *Senior Member, IEEE*, Ramon Villarino, David Girbau, *Senior Member, IEEE*

[1]

***Abstract*— A novel depolarizing chipless RFID tag is employed to estimate the variation of the dielectric properties of materials. The tag, comprising two 45-degree tilted dipoles printed on a thin substrate, is accommodated on top of the target material and it is interrogated wirelessly at radio frequency with a narrowband signal. Once interrogated, the tag radiates back a frequency selective response in cross-polarization. The depolarizing property of the tag allows to employ it on materials characterized by arbitrary large size thus avoiding the conceling effect of the large radar echo of the platform. The properties of the target material are estimated by resorting to the amount of frequency shift detected on the backscattered signal. The operation principle of the tag is initially illustrated by using simulations and then measurements are performed on various materials to show the reliability of the proposed procedure.**

***Index Terms*— Radio Frequency Identification (RFID), Chipless RFID, Permittivity Sensor, Frequency Selective Surfaces (FSS).**

I. Introduction

Sensing environmental parameters is a fundamental task that determines the success of a huge number of automated processes in real life. The sensing is usually performed indirectly, that is, an environmental change produces an detectable electrical difference in a circuit. A crucial component for the design of a sensor is represented by the transducer which converts the physical phenomenon to be monitored in an electrical variation. Although the large majority of sensors are based on a DC circuit [1], radio frequency sensors represent an innovative interesting solution. In this case, the change in the parameter can be monitored wirelessly by connecting antennas to an electronic circuit or by designing a sensing mechanism acting directly at radio frequency. The former approach is usually employed in RFID sensors [2]. Instead, in the latter case is the case of chipless RFID sensors [3].

One of the first examples of chipless RFID sensors is provided in [4] where a chipless RFID sensor for temperature is realized by using three functional layers of magnetic materials. Another solution consists in using Surface Acoustic Wave (SAW)-based sensors [5] for the wireless temperature and pressure monitoring. The Relative Humidity (RH) variation is also monitored by using chipless tags [3], [6], [7].

The aim of this paper is to sense wirelessly the dielectric properties of materials with an arbitrary shape and geometry. The application belongs to the non-destructive testing (NDT) methods and it is a novel scenario for chipless tags. A passive radio frequency label is attached on an object to estimate the electric properties of the object and eventually to monitor their change during time. The change of electric properties can be then correlated to relative humidity level [3]. A specific depolarizing chipless tag based on a couple of tilted dipoles is designed on a single layer thin substrate. The tag operates in cross-polarization to guarantee the needed isolation from RCS response of structural objects.

II. Sensing Mechanism and Tag Configuration

The idea is to attach a chipless tag on top of a surface for estimating the permittivity change based on the RF cross-polar response. The sensing mechanism is based on the measurement of the resonance frequency shift as a function of the material permittivity to be sensed. The tag operates in cross-polarization, which is a crucial feature for isolating the backscattered signal from the strong RCS response (mainly in co-polar) of the investigated object. The investigated sensing scenario and the layout of the proposed chipless resonator is displayed in Fig. 1. The tag is composed by N x N unit cells. The optimal number of unit cells will be determined later. The simulations are initially performed for a periodic resonator by using a proprietary MoM code. The resonator is formed by a couple of dipoles oriented obliquely with respect to the incident field orientation. The tag is printed on a 32 mil thick Rogers 4003 substrate.

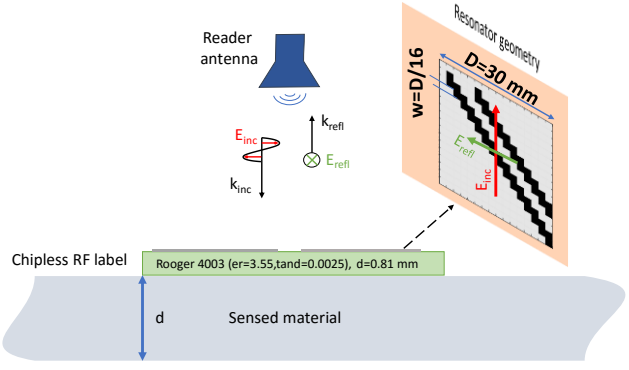

Fig. 1 –Sensing scenario and layout of the proposed chipless tag.

[1] Manuscript received September 30th 2017.

This work was supported by the, H2020 Grant Agreement 645771–EMERGENT. F. Costa, A. Gentile, L. Buoncristiani, S. Genovesi are with Department of Information Engineering, University of Pisa, 56122 - Pisa, Italy. E-mail:filippo.costa@iet.unipi.it. A. Lazaro, D.Girbau, R. Villarino are with the Department of Electronics, Electrics and Automatic Control Engineering, Rovira i Virgili University, Tarragona, 43007 Tarragona, Spain. e-mail: antonioramon.lazaro@urv.cat.

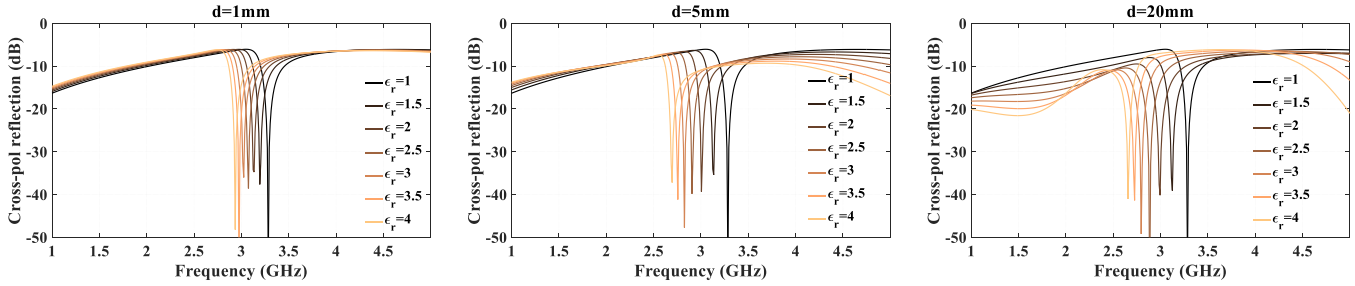

(a) (b) (c)

Fig. 2 – Cross-polar reflection coefficient of an infinite FSS structure with the layout reported in Fig. 1 for various thickness of the sensed material located behind the tag. (a) d=1 mm, (b) d=5 mm, (c) d=20 mm.

The reflection coefficient of the resonator presents two maxima in the cross-polar response and a deep and high-Q null in between. The sharp null moves as a function of the permittivity of the sensed material. The frequencies associated with the maxima are located where each dipole length becomes equal to a half-wavelength calculated in the effective medium composed by the air, the substrate of the tag and the material to be sensed. In this case the length of the two dipoles has been chosen equal to $l_1 = \sqrt{2}15/16\,D = 39.7mm$ and $l_2 = \sqrt{2}11/16\,D = 29.2mm$, where D represents the periodicity of the FSS and has been set to 30 mm. The two dipoles resonator can be modelled with a couple of LC series circuits connected in parallel [8], [9]. When the resonator is loaded with the sensed material, the values of capacitances change proportionally to the value of the effective permittivity ($\varepsilon_{eff}C_0$) (where C_0 is the freestanding capacitance value and ε_{eff} is the effective capacitance of the effective medium) with a consequent reduction of the resonance frequency f_0 by a factor $f_0/\sqrt{\varepsilon_{eff}}$. If the thickness of the sensed material is lower than half FSS periodicity, its effective permittivity is thickness dependent [8], [10]. An example of the cross-polar reflection response of the resonator in a periodic environment as a function of the permittivity value and the thickness of the sensed material is reported in Fig. 2. When the ratio of thickness of the sensed material over the resonator size exceeds a certain value [8], a saturation of the frequency shift is achieved since the electric field is entirely confined inside the sensed material. The field penetration behavior is pictorially represented in Fig. 3. This means that the sensing mechanism is related to the size of the resonator. The larger is the size of the resonator, the deeper is the penetration of the sensing.

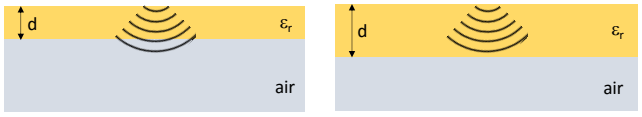

(a) (b)

Fig. 3 – Penetration depth of the electromagnetic field in the sensed material.

The frequency shift achieved with the two-dipoles sensor as a function of the substrate thickness and for different dielectric permittivity values of the material is reported in Fig. 4. The effect of losses in the sensed material is also analyzed in Fig. 5. As it is evident, a moderate dielectric loss does not create problems in the detection of the peak. Finally, the truncated version of the resonator is simulated by using Ansys Electronics v. 16.

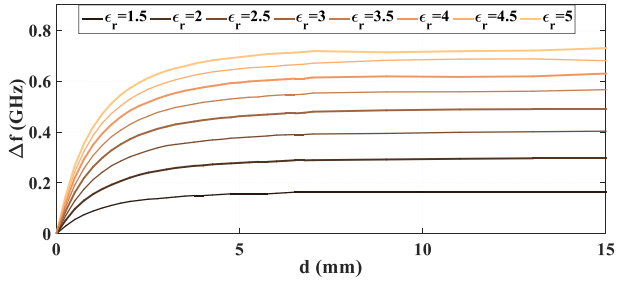

Fig. 4 – Delta frequency shift (Δf) of the resonance peak with respect to the initial value as a function of the thickness d of the sensed material and for different values of its permittivity.

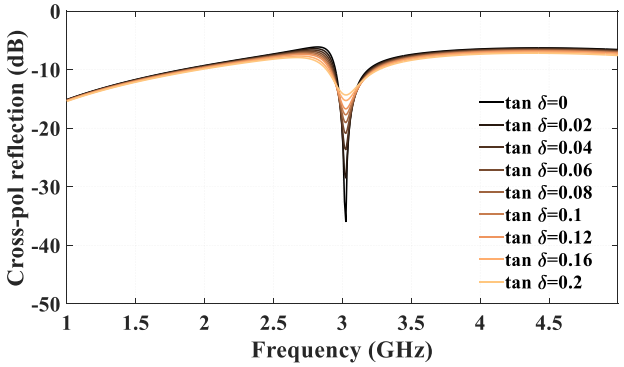

Fig. 5 – Effect of losses in the sensed material. Simulations for a sensed material having ε_r = 3 and a thickness of d=1 mm.

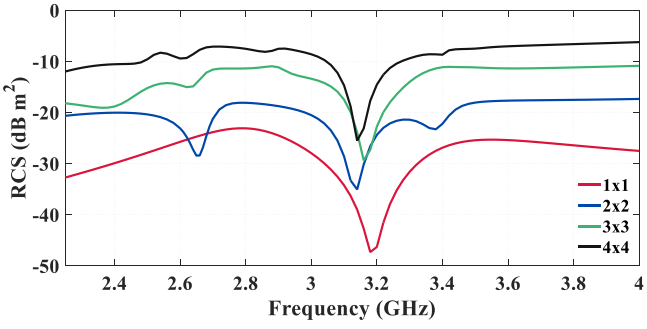

Fig. 6 – Radar cross section of the finite size FSS as a function of the number of unit cells N.

Several configurations have been simulated: 1x1, 2x2, 3x3 and 4x4 unit cells. The increase of the number of unit cells leads to an increased RCS level and thus facilitates the tag detection. Looking at the simulated RCS in Fig. 5, we can notice that the 2x2 configuration is characterized by a couple of spurious peaks (confirmed also with measurements) and thus we decided to report experimental results of the 1x1 and 3x3 tags.

III. Experimental Validation

The sensing method has been tested in a semi-anechoic environment. Two Vivaldi antennas have been used to interrogate the tag. The distance from the antennas and the tag is 40 cm for the 1x1 tag and 60 cm for the 3x3 tag. Initially, the background measurement is performed for the calibration [11] (this signal is subtracted from signals in presence of the tag). Afterwards, several materials have been placed behind the tag and the frequency response is measured as shown in Fig. 7 both for the 1x1 and for the 3x3 tags. Additional tests on materials characterized by a large footprint have been also performed. In particular, the chipless tag has been attached on top two thick and large sized pieces of woods and some relative frequency shift is observed. The measured cross-polar RCS is shown in Fig. 8.

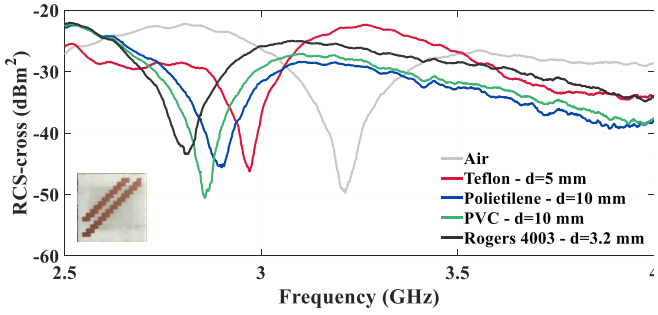

(a)

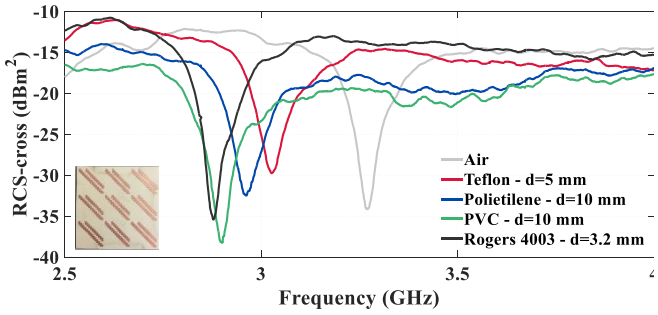

(b)

Fig. 7 – Measured cross-pol RCS for different kind of materials placed behind the resonator. (a) 1x1 tag, (b) 3x3 tag. Fabricated tags are shown in the inset of the figures.

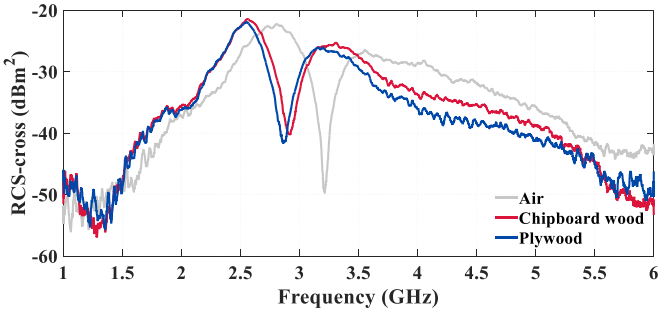

Fig. 8 – Measured cross-polar RCS of the tag placed on two different large and thick pieces of wood. (a) chipboard wood (b) plywood.

A summary of the measured and simulated frequency shift is reported in Table 1. The agreement between measurements and simulations is satisfactory considering that the permittivity is measured wirelessly in a non-controlled electromagnetic environment. The main source of error in determining the permittivity of the material behind the tag in the lab is related to the manual positioning of the tag which can cause the presence of an air gap between the material to be sensed and the substrate of the chipless tag. An air gap of 0.1 mm can induce a frequency shift as high as 100 MHz and thus determining an uncertainty in the order on 15% in the estimation of the permittivity. However, it is worth underlining that the fundamental idea of this work is not to present a new measurement setup for dielectric permittivity estimation but is to propose a passive device for monitoring the variation of a target material during time. For this reason, the presence of air gaps and positioning errors is not a real issue.

Table 1 – Summary of the frequency shifts achieved with the measured materials. Frequency f_0 and Δf are expressed in GHz.

Material	d [mm]	f_0 (3x3)	f_0 (1x1)	Δf (3x3)	Δf (1x1)	Δf sim.
Air		3.27	3.21	-	-	-
Teflon	5	3.027	2.97	0.243	0.24	0.275
Polietilene	10	2.98	2.9	0.29	0.31	0.35
PVC	10	2.9	2.85	0.37	0.36	0.4
Rogers 4003	3.2	2.89	2.81	0.38	0.4	0.45
Clipboard wood	10	2.98	2.92	0.29	0.29	-
Plywood	10	2.85	2.86	0.42	0.35	-

IV. Conclusion

A wireless method for estimating the dielectric properties of objects has been presented. A completely passive depolarizing label is designed and placed on objects. The cross-polar RCS has been measured up to a distance of 60 cm.

References

[1] Z. Chen and C. Lu, "Humidity Sensors: A Review of Materials and Mechanisms," *Sens. Lett.*, vol. 3, no. 4, pp. 274–295, Dec. 2005.

[2] L. Su, J. Mata-Contreras, P. Vélez, and F. Martín, "A Review of Sensing Strategies for Microwave Sensors Based on Metamaterial-Inspired Resonators: Dielectric Characterization, Displacement, and Angular Velocity Measurements for Health Diagnosis, Telecommunication, and Space Applications," *International Journal of Antennas and Propagation*, 2017.

[3] R. R. Fletcher and N. A. Gershenfeld, "Remotely interrogated temperature sensors based on magnetic materials," *IEEE Trans. Magn.*, vol. 36, no. 5, pp. 2794–2795, Settembre 2000.

[4] W. Buff, S. Klett, M. Rusko, J. Ehrenpfordt, and M. Goroli, "Passive remote sensing for temperature and pressure using SAW resonator devices," *IEEE Trans. Ultrason. Ferroelectr. Freq. Control*, vol. 45, no. 5, pp. 1388–1392, Sep. 1998.

[5] R. S. Nair, E. Perret, S. Tedjini, and T. Baron, "A Group-Delay-Based Chipless RFID Humidity Tag Sensor Using Silicon Nanowires," *IEEE Antennas Wirel. Propag. Lett.*, vol. 12, pp. 729–732, 2013.

[6] E. M. Amin, M. S. Bhuiyan, N. C. Karmakar, and B. Winther-Jensen, "Development of a Low Cost Printable Chipless RFID Humidity Sensor," *IEEE Sens. J.*, vol. 14, no. 1, pp. 140–149, Jan. 2014.

[7] M. Borgese, F. A. Dicandia, F. Costa, S. Genovesi, and G. Manara, "An Inkjet Printed Chipless RFID Sensor for Wireless Humidity Monitoring," *IEEE Sens. J.*, vol. 17, no. 15, pp. 4699–4707, Aug. 2017.

[8] F. Costa, A. Monorchio, and G. Manara, "An Overview of Equivalent Circuit Modeling Techniques of Frequency Selective Surfaces and Metasurfaces," *Appl. Comput. Electromagn. Soc. J.*, vol. 29, no. 12, pp. 960–976, 2014.

[9] M. Garcia-Vigueras, F. Mesa, F. Medina, R. Rodriguez-Berral, and J. L. Gomez-Tornero, "Simplified Circuit Model for Arrays of Metallic Dipoles Sandwiched Between Dielectric Slabs Under Arbitrary Incidence," *IEEE Trans. Antennas Propag.*, vol. 60, no. 10, pp. 4637–4649, Oct. 2012.

[10] D. Girbau, A. Lázaro, and R. Villarino, "Passive wireless permittivity sensor based on frequency-coded chipless RFID tags," in *2012 IEEE/MTT-S International Microwave Symposium*, 2012, pp. 1–3.

[11] F. Costa, S. Genovesi, and A. Monorchio, "A Chipless RFID Based on Multiresonant High-Impedance Surfaces," *IEEE Trans. Microw. Theory Tech.*, vol. 61, no. 1, pp. 146–153, Jan. 2013.